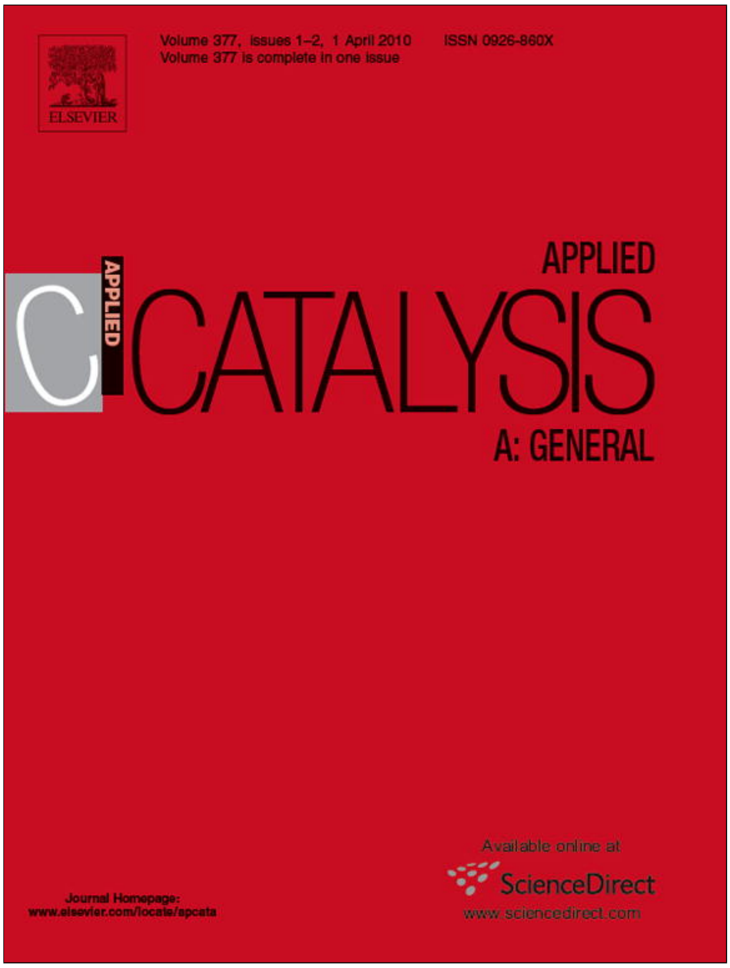

Volume 377, issues 1–2, 1 April 2010 ISSN 0926-860X
Volume 377 is complete in one issue

ELSEVIER

APPLIED CATALYSIS A: GENERAL

Available online at ScienceDirect www.sciencedirect.com

Journal Homepage: www.elsevier.com/locate/apcata

Applied Catalysis A: General 377 (2010) 140–149

Contents lists available at ScienceDirect

Applied Catalysis A: General

journal homepage: www.elsevier.com/locate/apcata

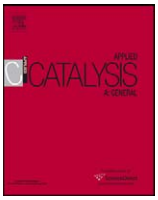

Adsorbent as an essential participant in photocatalytic processes of water and air purification: Computer simulation study

D.S. Selishchev[a], P.A. Kolinko[b], D.V. Kozlov[b,*]

[a] Novosibirsk State University, Novosibirsk 630090, Russian Federation
[b] Boreskov Institute of Catalysis, pr. ak. Lavrentieva, Novosibirsk 630090, Russian Federation

A R T I C L E I N F O

Article history:
Received 17 August 2009
Received in revised form 18 January 2010
Accepted 19 January 2010
Available online 25 January 2010

Keywords:
Photocatalysis
Titanium dioxide
Adsorption
Activated carbon
Reaction kinetics simulation

A B S T R A C T

The influence of adsorbent on the kinetics of (photo)catalytic oxidation processes was studied using the simple single and double stage reaction mechanisms with the adsorption stages corresponding to Langmuir model. It was found that in the static reactor in all cases the usage of adsorbent leads to the prolongation of substrate (*A*) removal and product (*P*) accumulation kinetic curves but the substrate concentration becomes lower during almost all (photo)catalytic process. Fitting of experimental data points of acetone photocatalytic oxidation reaction demonstrated a good correlation with proposed reaction mechanism. Calculated adsorption constants values are close to those reported in literature.

The using of adsorbent in flowing conditions leads to the decrease of maximum outlet substrate concentration in the case if the inlet substrate concentration is too high to be oxidized completely for one run.

Kinetics simulation in the case of (photo)catalytic reaction with intermediate demonstrates that adsorbent could accumulate additional intermediate quantity thus keeping catalyst surface more active and contributing to faster substrate (*A*) removal.

1. Introduction

Methods of photocatalytic purification of water and air have been extensively developed over last decades [1–4]. Main efforts are focusing on the synthesis of highly active photocatalysts which are usually based on the anatase form TiO_2. Popular commercial photocatalysts such as Degussa P25 (Degussa AG) and Hombikat UV-100 (Sachtleben Chemie GmbH) already became as a reference samples for many researchers because they posses very high activity in water (P25) and air (Hombikat UV-100) photocatalytic treatment processes.

At the same time adsorption properties of the photocatalytic system also influence on the rate of photocatalytic processes especially in the low concentration region which is obvious from the classic Langmuir–Hinshelwood (L.–H.) dependence of the product formation rate on the gas concentration of a substrate:

$$\frac{dP}{dt} = \frac{kK_aA}{1+K_aA} \xrightarrow[K_aA \ll 1]{} \frac{dP}{dt} \approx kK_aA. \tag{1}$$

In this case the rate of photooxidation is in direct proportion to the adsorption constant K_a. Probably it is a reason of constantly growing interest to the combination of adsorption and photocatalysis in last years.

Sauer and Ollis [5] and later Vorontsov and Savinov [6] demonstrated the influence of adsorbed substrate quantity on the kinetics of photocatalytic reaction. Maurette et al. [7] prepared TiO_2/zeolite photocatalyst and tested it in the reaction of butanol photocatalytic oxidation (PCO) in a continuous flow annular reactor in 2003. Authors periodically switched off and on the UV-lamp thus changing the adsorption and PCO modes of operation of the reactor thus investigating the rate of adsorption and the rate of PCO separately. Probably if authors switched on and off the inlet substrate supply keeping the UV-lamp constantly working they would achieve more informative result because they would measure the competition between adsorption and PCO in such case.

In the same 2003 year Shiraishi et al. [8] became closer to practice and reported results about treatment of gaseous formaldehyde in a small chamber using a photocatalytic reactor combined with a continuous adsorption/desorption apparatus. Later Ollis and co-workers [9] perfectly explained results obtained by Shiraishi assumed that the reaction following a L.–H. rate form and taking into account the temperature dependence of adsorption and rate constants. Other researchers [10] immobilized TiO_2 on an activated carbon (TiO_2/AC) filter installed in a commercial air cleaner and tested it in the PCO of NO and toluene ppb level

---

[*] Corresponding author. Tel.: +7 383 3331617.
E-mail address: kdv@catalysis.ru (D.V. Kozlov).

0926-860X/$ – see front matter © 2010 Elsevier B.V. All rights reserved.
doi:10.1016/j.apcata.2010.01.030

Table 1
Examples of TiO_2 mixing with adsorbents and the corresponding beneficial effects.

TiO_2/adsorbent system	Test PCO reaction	Beneficial effect	Ref.
TiO_2/AC a mechanical mixture	4-Chlorophenol in aqueous suspension	Increased rate of substrate disappearance and lower intermediate concentration.	[15]
TiO_2/AC a mechanical mixture	Phenol in aqueous suspension	Decrease of photocatalyst deactivation rate during three consecutive runs.	[16]
TiO_2/MOR a mechanical mixture MOR = $[(CaK_2Na_2)(AlSi_5O_{12})_2 \times 6H_2O]$ mordenite zeolite	Gaseous acetaldehyde in O_2	About 1.3 times increased CO_2 formation for 1 h of PCO if to compare with the separated TiO_2 and MOR.	[17]
TiO_2/Nafion	Paraquat (herbicide) in aqueous solution	Increased rate of substrate disappearance in the presence of phosphate and sulphate anions which promote the substrate adsorption	[18]

removal. Authors demonstrated better pollutants removal with the TiO_2/AC system then with only TiO_2 but did not measure the final products (like CO_2) accumulation. They also conducted only static experiments in a chamber whereas continuous flow experiments could give the better information about practical usefulness of TiO_2/AC system.

A lot of adsorbents were used to modify TiO_2 some of them are summarized in Table 1.

Several questions still remained after literature inspection. Which characteristic of TiO_2/adsorbent system efficiency is more appropriate – rate of substrate disappearance or product formation? Where the benefits of adsorbent use are more pronounced – in flow or static conditions? How the PCO reactions with different mechanisms are liable to the adsorbent influence? Answers to these questions were the subject of current study.

It should be mentioned also before one will begin to read this paper that all adsorption stages are supposed to be equilibrium describing by Langmuir isotherm. Authors do not aim to describe precisely the reaction mechanisms, including chemisorptions, mass transfer and primary reactions on the photocatalyst surface. Authors also do not intend to describe dependences of reaction parameters (rate and adsorption constants) on light intensity like it was done by Ollis with co-workers in Refs. [11,12] because the main purpose of current work was to reveal the role of adsorbent and to develop approach for describing kinetics of (photo)catalytic reactions complicated with the secondary adsorption processes.

2. Simple single-stage PCO reaction

The following section describes the single-stage kinetic model development in static and flow reactors. It is supposed that the substrate (A) adsorbs on the catalyst and adsorbent whereas product (P) exists only in gaseous[1] state.

2.1. Static reactor

Let us consider the mechanism of single-stage (photo)catalytic reaction with reversible substrate adsorption according to the Langmuir mechanism (S.1):

$$\begin{aligned} &1.\, A + z_1 \overset{K_{a1}}{\rightleftarrows} Az_1 \\ &2.\, A + z_2 \overset{K_{a2}}{\rightleftarrows} Az_2 \\ &3.\, Az_1 \xrightarrow{k} \alpha P + z_1 \end{aligned} \tag{S.1}$$

It is supposed that one substrate molecule is converted into α product molecules. For example one acetaldehyde molecule gives two CO_2 molecules in the case of complete PCO reaction so $\alpha = 2$ for this reaction.

Taking into account that the total initial amount of substrate is distributed between gas phase in the form of substrate or product and surfaces of photo(catalyst) and adsorbent and also using the rate expression for the stage 3 (S.1) the following system of equations could be suggested:

$$A_0 V = AV + \frac{PV}{\alpha} + S_\Sigma (C_{a1} + C_{a2}) \tag{2}$$

$$\frac{dP}{dt} = \alpha k \frac{S_\Sigma}{V} C_{a1} \tag{3}$$

$$C_{a1} = \frac{C_1 K_{a1} A}{1 + K_{a1} A} \tag{4}$$

$$C_{a2} = \frac{C_2 K_{a2} A}{1 + K_{a2} A} \tag{5}$$

$$S_\Sigma = \frac{N_1}{\beta_1} + \frac{N_2}{\beta_2}, \tag{6}$$

here S_Σ is the total surface area of the mixed catalyst/adsorbent system. $C_1 = N_1/S_\Sigma$ and $C_2 = N_2/S_\Sigma$ are the concentrations of catalyst active sites and adsorbent adsorption sites correspondingly. C_{a1} and C_{a2} are the current concentrations of adsorbed substrate on the catalyst and adsorbent correspondingly. It was possible to solve the system (2)–(5) in terms of surface coverage $\Theta_{a1} = C_{a1}/C_1$ and $\Theta_{a2} = C_{a2}/C_2$ but in the special case of $N_2 = 0$ (mol) will be obtained non-zero values of Θ_{a2} which is not good from the physical point of view.

If we substitute Eq. (4) and (5) into Eq. (2) then differentiate it with respect to time and substitute Eq. (3) into the result then we finally could obtain the differential equation in substrate concentration $A(t)$:

$$\frac{dA}{dt} = -\frac{k(S_\Sigma/V)C_1(K_{a1}A/(1+K_{a1}A))}{1 + (S_\Sigma/V)\Big((C_1K_{a1}/(1+K_{a1}A)^2) + (C_2K_{a2}/(1+K_{a2}A)^2)\Big)}. \tag{7}$$

In spite of that Eq. (7) could be solved analytically but the substrate concentration dependence on time $A(t)$ will be in implicit form and still hard to analyze. For this reasons we solved all differential equations numerically by the fourth-order Runge-Kutta method in the program *MathCad* (*Mathsoft Engineering & Education, Inc.*).

2.2. Initialization of parameters

The following values of initial parameters were chosen for the case of acetone vapor PCO before starting the simulation of Eq. (7) (Table 2). If both masses (m_1) and (m_2) will be equal to 0.01 g then the initial amounts of catalyst and adsorbent could be calculated as: $N_1 = S_{1BET}\beta_1 m_1$ and $N_2 = S_{2BET}\beta_2 m_2$. Thus the starting parameters for kinetics simulation are $N_1 = 2.9 \times 10^{-5}$ mol, $N_2 = 2.2 \times 10^{-5}$ mol, $S_\Sigma = (11.5 \text{ or } 3.5)\ m^2$ if to simulate the kinetics with or without adsorbent.

According to our previous results [13] the acetone quantity equal to 1000 ppm ($A_0 = 4 \times 10^{-5}$ mol l^{-1}) could be completely photooxidized in a static reactor of $V = 0.5$ l volume with 0.01 mg TiO_2 for the time ≈2 h. Taking this fact into account the rate constant value was chosen as $k = 0.004\ s^{-1}$ and it is the only parameter which could

---

[1] Here and hereafter "gas" could be replaced by "liquid".

Table 2
Values of initial parameters, used for the acetone vapor kinetics simulation according to Eq. (7).

Parameter	Value in Ref.	Recalculated value for use in current simulation	Ref.
β_1	$5\times10^{14}\,\mathrm{cm}^{-2}$	$8.3\times10^{-6}\,\mathrm{mol\,m}^{-2}$	[19]
β_2	0.13 g-aceton g-carbon^{-1}	$2.8\times10^{-6}\,\mathrm{mol\,m}^{-2}$	[20]
$S_{1\mathrm{BET}}$	$350\,\mathrm{m}^2\,\mathrm{g}^{-1}$		From manufacturer for Hombukat UV-100
$S_{2\mathrm{BET}}$	$800\,\mathrm{m}^2\,\mathrm{g}^{-1}$		[20]
K_{a1}	$1.2\times10^{-4}\,\mathrm{ppm}^{-1}$ (40 °C)	$1\times10^{4}\,\mathrm{L\,mol}^{-1}$ (corrected for 30 °C)	[21]
K_{a2}	$4\times10^{-3}\,\mathrm{ppm}^{-1}$ (30 °C)	$1\times10^{5}\,\mathrm{L\,mol}^{-1}$	[20]

not be found in the literature because it depends on the specific experimental conditions (light intensity, humidity, illuminated area, spectral characteristics of light source, etc.)

2.3. Kinetics in static reactor

Calculated kinetic curves for gas phase and surface are presented in Figs. 1 and 2 correspondingly. Two cases are simulated: (1) there is only (photo)catalyst in the system; (2) there are (photo)catalyst and adsorbent in the system.

The initial concentration of substrate is lowered by the value of $\Delta A_0 = 1.25\times10^{-5}\,\mathrm{mol\,l}^{-1}$ or $\Delta A_s = 2.9\times10^{-5}\,\mathrm{mol\,l}^{-1}$ if compare with the total initial concentration $A_0 = 4\times10^{-5}\,\mathrm{mol\,l}^{-1}$. It means that about 31% and 73% of substrate are totally adsorbed in the beginning of PCO on the surface of catalyst and adsorbent in the first and second cases. So the first benefit from adsorbent usage is the lowering of initial substrate concentration which could be useful if the substrate is a toxic species.

On the other hand there exist a cross-point time $t_s \approx 1200$ s (Fig. 2) when the catalyst surface coverage become equal in the first and second cases and the gaseous substrate concentration become higher in the case of adsorbent presence in the system. More over adsorbent presence leads to the prolongation of all kinetic curves and lowering the product (P) accumulation rate (Fig. 1). P is usually nontoxic species like CO_2 and H_2O and prolonged kinetic is inessential at the same time the substrate (A) could be so toxic (like HCN) that even small excess for a long time could be dangerous. And this is the main disadvantage of adsorbent usage in this case. Vorontsov and Savinov [6] in 1998 simulated the influence of non-irradiated surface on the PCO kinetics and obtained the similar result because non-irradiated catalyst surface could be considered as adsorbent.

It is easy to calculate the apparent rate constant of the above PCO reaction if to approximate it with the simple first-order kinetic low:

$$\frac{dA}{dt} = -k'A. \tag{8}$$

If one will equal right-hand sides of Eq. (7) and (8) then for the case of low substrate concentration (i.e. $K_{a1}A \ll 1$ and $K_{a2}A \ll 1$) he will obtain the following expression for the apparent first-order constant k':

$$k' = \frac{k(S_\Sigma/V)C_1K_{a1}}{1+(S_\Sigma/V)(C_1K_{a1}+C_2K_{a2})} \xrightarrow[N_i=S_\Sigma C_i(i=1,2)]{} \frac{k}{1+(V/N_1K_{a1})+(N_2K_{a2}/N_1K_{a1})}. \tag{9}$$

The same apparent first-order constant k'' without adsorbent ($N_2 = 0$) is equal:

$$k'' = \frac{k}{1+(V/N_1K_{a1})}, \tag{10}$$

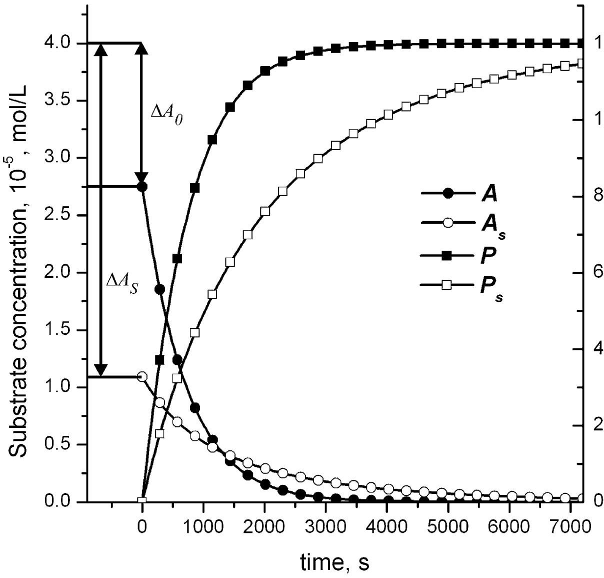

Fig. 1. The adsorbent effect on the kinetics of gaseous substrate (A) removal and product (P) accumulation in a 0.5 l static reactor. A and P are the substrate and product kinetic curves in the system with only (photo)catalyst ($m_1 = 0.01$ g); A_s and P_s are the same curves but in the system with addition of adsorbent ($m_2 = 0.01$ g). Initial substrate concentration without taking into account the initial adsorption is equal $A_0 = 4\times10^{-5}\,\mathrm{mol\,l}^{-1}$, $k = 0.004\,\mathrm{s}^{-1}$, $\alpha = 3$, all other parameters were taken from Table 2.

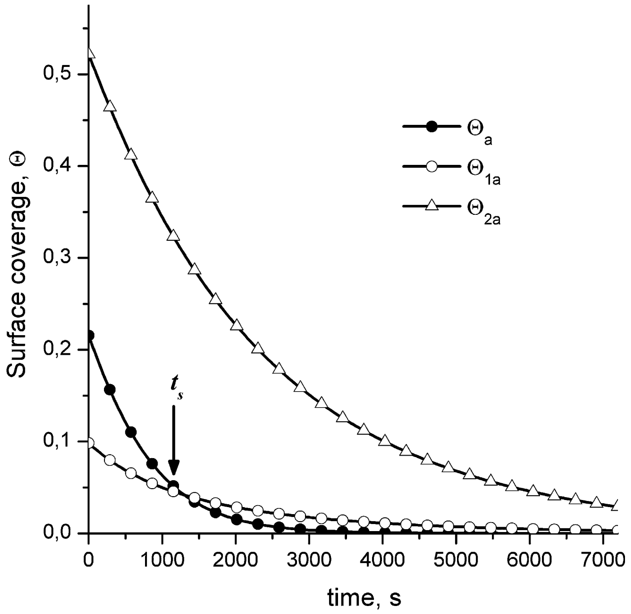

Fig. 2. The adsorbent effect on the kinetics of adsorbed substrate. $\Theta_a = C_a/C_1$ is the (photo)catalyst surface coverage by substrate molecules (Az_1) in the system with only (photo)catalyst; $\Theta_{a1} = C_{a1}/C_1$ and $\Theta_{a2} = C_{a2}/C_2$ are the catalyst (Az_1) and adsorbent (Az_2) surface coverage correspondingly in the system with addition of adsorbent. In the first case $C_1 = 8.3\times10^{-6}$ and $C_2 = 0\,\mathrm{mol\,m}^{-2}$; in the second case $C_1 = 2.5\times10^{-6}$ and $C_2 = 1.9\times10^{-6}\,\mathrm{mol\,m}^{-2}$. All other parameters are the same as in the caption in Fig. 1.

and their ratio will be:

$$\frac{k''}{k'} = 1 + \frac{N_2 K_{a2}}{V + N_1 K} = 1 + \gamma N_2 \Rightarrow \frac{k'}{k''} = \frac{1}{1 + \gamma N_2}. \qquad (11)$$

It is obvious from Eq. (10) that even without adsorbent with the same (photo)catalyst quantity the apparent first-order rate constant k'' is decreasing with the reactor volume (V) increase. Eq. (11) demonstrates that in the system with adsorbent and with the same irradiated catalyst quantity the apparent constant k' is decreasing with the increase of the adsorbent quantity (N_2). In the case shown in Fig. 1 the ratio k'/k'' = 3.78 and it means that the effective reaction time with the adsorbent becomes 3.78 times longer in the low substrate concentration range.

2.4. Fitting of experimental data

Analytic solution of Eq. (7) could be used for the fitting of experimental data in order to prove the accuracy of reaction mechanism (S.1). A cylindrical photocatalytic reactor with removable adsorbent layer is presented in Fig. 3. This reactor was installed in a V = 404 l plastic chamber which was isolated from environment and equipped with injector for reagent injection and gas phase monitoring. The reactor was equipped with ventilator to provide air flow passing through the photocatalytic and adsorption layers with the 60 m^3 h^{-1} flow rate.

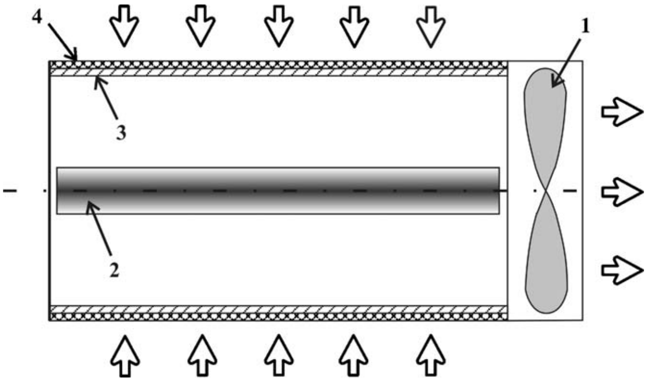

Fig. 3. Cylindrical photocatalytic reactor with adsorbent. (1) ventilator; (2) UV-lamp (Philips CLEO 15 W); (3) transparent support with photocatalyst (TiO$_2$ powder Hombikat UV100, $m_1 \sim 1.5$ g); (4) removable air-conducting nonwoven material with supported adsorbent (activated carbon, $S_{BET} \sim 800$ m^2 g^{-1}, $m_2 \sim 2$ g). Arrows indicate the air flow direction.

In the first experiment mass transfer limitations were checked (Fig. 4). The initial rate of CO$_2$ accumulation during acetone vapor photooxidation with the same initial amount of acetone vapor was measured as a function of air flow through the reactor. In this experiment only photocatalytic filter without adsorbent was used. It can be seen from Fig. 4 that in flow rate range 5.3–116 m^3 h^{-1} the initial CO$_2$ accumulation rate (W_{CO_2}) is practically independent on the flow rate taking into account 5% relative error of W_{CO_2} measurement. It means that in our experimental conditions only kinetics determine the photocatalytic oxidation rate but not mass transfer and we could easily apply reaction mechanism (S.1) with the corresponding equations to fit the experimental data.

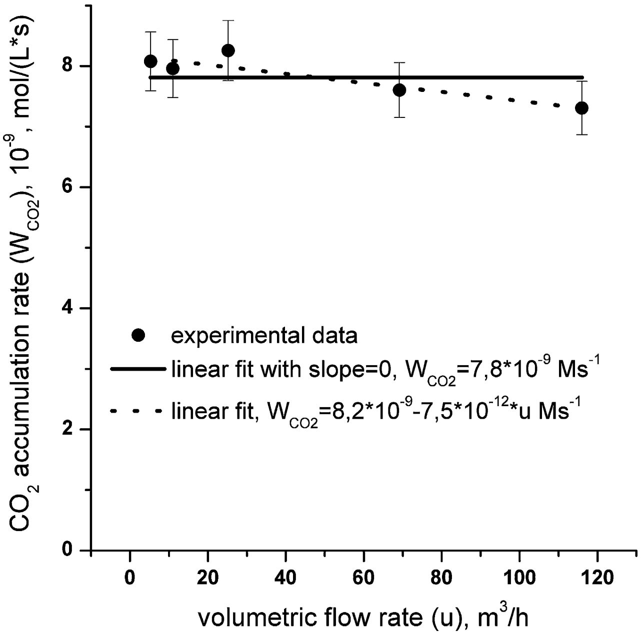

Fig. 4. Dependence of initial CO$_2$ accumulation rate on the volumetric gas mixture flow rate through the cylindrical photocatalytic reactor (Fig. 3) placed in 404 l isolated plastic chamber during acetone vapor photocatalytic oxidation.

In the beginning of second experiment the 0.5 cm^3 amount of liquid acetone was injected into the chamber. If to neglect acetone adsorption then its initial vapor concentration should be at the $A_0 = 1.65 \times 10^{-5}$ mol l^{-1} level. UV-lamp was turned on immediately after the acetone evaporation. Acetone and CO$_2$ concentrations were monitored by the periodic chromatographic analysis of reaction gas mixture. This experiment was conducted twice: for the first time in the presence of only photocatalyst (TiO$_2$ Hombikat UV100, $m_1 \sim 1.5$ g); and for the second time in the presence of both photocatalyst and adsorbent (activated carbon $m_2 \sim 2$ g). Experimental results and their fitting are presented in Fig. 5.

Solid lines in Fig. 5 correspond to fitting of acetone concentration profiles with integrated form of Eq. (7). Fitting of the acetone concentration decrease for the first time resulted in values of rate constant (k), acetone adsorption on TiO$_2$ constant (K_{a1}) and the number of TiO$_2$ active (adsorption) sites (N_1). They are $k = 7.5 \times 10^{-4}$ s^{-1}, $K_{a1} = 3.1 \times 10^5$ l mol^{-1} and $N_1 = C_1 S_\Sigma = 2.5 \times 10^{-3}$ mol. Taking into account values of β_1 and S_{1BET} from Table 2 the TiO$_2$ mass could be calculated as $m_1 = N_1/(\beta_1 S_{1BET})$ = 0.86 g. The deviation of this calculated value from real known mass

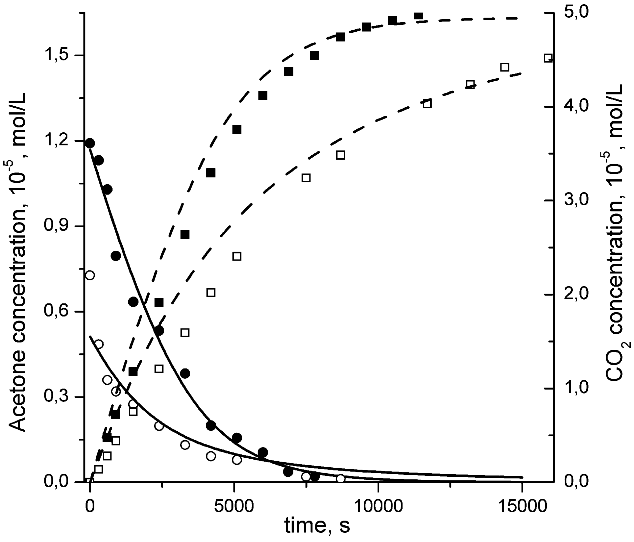

Fig. 5. Fitting results of acetone photocatalytic oxidation in a 404 l isolated plastic chamber. (●) Acetone vapor and (■) CO$_2$ concentration profiles during the acetone photocatalytic oxidation with the reactor (Fig. 3) equipped with only photocatalyst. (○) Acetone vapor and (□) CO$_2$ concentration profiles in the case of reactor equipped with photocatalyst and adsorbent. Initial amount of injected liquid acetone equals 0.5 cm^3.

of used photocatalyst is not big and could be explained by difference between current TiO_2 parameters ($\beta_1, S_{1BET}, K_{a1}$) and those reported in literature [19]. Fitting of acetone kinetic curve obtained for the second time using the known parameters k, K_{a1} and N_1 gives us the adsorbent characteristics $K_{a2} = 1.2 \times 10^6$ l mol^{-1} and $N_2 = 3.6 \times 10^{-3}$ mol. Both fitted curves are close to experimental points indicating a good agreement with the model.

Dashed lines in Fig. 5 correspond to CO_2 accumulation kinetic curves were calculated from acetone concentration decrease data (solid lines in Fig. 5) and mass balance taking into account adsorption. Both theoretical CO_2 formation curves are laying slightly above corresponding experimental CO_2 data points. Probably it is explaining by formation of a small amount of intermediate (like acetic acid) and its underestimation in total mass balance. Nevertheless, a good agreement of these curves with experimental points also speaks in favor of the model (S.1).

Matos et al. [14] investigated phenol and other aqueous organic pollutants photocatalytic degradation in water suspension with addition of TiO_2 Degussa P25 and two types of activated carbon (AC) with about 100 times different adsorption constants against phenol. They measured kinetic curves of phenol disappearance and approximated them with first-order kinetic low with corresponding estimation of first-order apparent kinetic constant (k_{app}).

The AC purchased from Merck had very high adsorption constant and demonstrated synergistic effect, i.e. k_{app} was higher in the TiO_2/AC suspension than in only TiO_2 containing suspension. Although this observation does not mean that the final photooxidation product – CO_2 – was formed faster in the TiO_2/AC system since authors did not measure it.

Another AC with the commercial name 'Purocarbon' had the adsorptivity against phenol comparable with TiO_2. Kinetic curves for its disappearance in TiO_2/AC and TiO_2 only water suspensions are presented in Fig. 6. Both lines are similar to theoretical and experimental kinetic curves of substrate removal reported in Figs. 1 and 5 indicating that in the case of reversible physical adsorption of the substrate its removal from purifying medium is slower in the presence of adsorbent.

In Table 3 of [14] authors report values of k_{app} as a function of TiO_2 quantity in water suspension. Eq. (10) and (9) could be used to derive linearized dependences of inverse k_{app} on the inverse TiO_2 quantity. For the case of only TiO_2 water suspensions it is Eq. (12) and for the case of TiO_2/AC water suspension it is Eq. (13):

$$\frac{1}{k_{\mathrm{app}}(\mathrm{TiO_2})} = \frac{1}{k} + \left(\frac{V}{kK_{a1}}\right) \cdot \frac{1}{N_1}, \tag{12}$$

$$\frac{1}{k_{\mathrm{app}}(\mathrm{TiO_2} - \mathrm{AC})} = \frac{1}{k} + \left(\frac{V}{kK_{a1}} + \frac{N_2 K_{a2}}{kK_{a1}}\right) \cdot \frac{1}{N_1}, \tag{13}$$

where N_1 proportional to TiO_2 mass.

The inset in Fig. 6 shows Matos et. al. experimental data (taken from Table 3 in [14]) in inverse coordinates: $(1/k_{\mathrm{app}}) - (1/\mathrm{m(TiO_2)})$. In such form it seems that both dependences are linear except for experiments with 75 mg TiO_2 quantity for both cases with and without AC (marked with circle and '?'). If one will do linear fit of both experimental data sets ignoring marked points than intercept of both lines with ordinate axis will be almost similar indicating that true kinetic constant (k) within the limits of mechanism (S.1) is equal $k = 1/176 = 5.7 \times 10^{-3}$ min^{-1}.

2.5. Flow reactor with perfect mixing

One of the features of adsorbent presence in static system is the decrease of substrate concentration during (photo)catalytic reactions. Let us examine if there exist any advantage of adsorbent presence in flow conditions. Flow reactor with perfect mixing is presented in Fig. 7. The reaction mechanism is the same as presented in (S.1). The contact time τ (s) is equal $\tau = V/u$, where V is reactor volume (l) and (u) is volumetric flow rate (l s^{-1}).

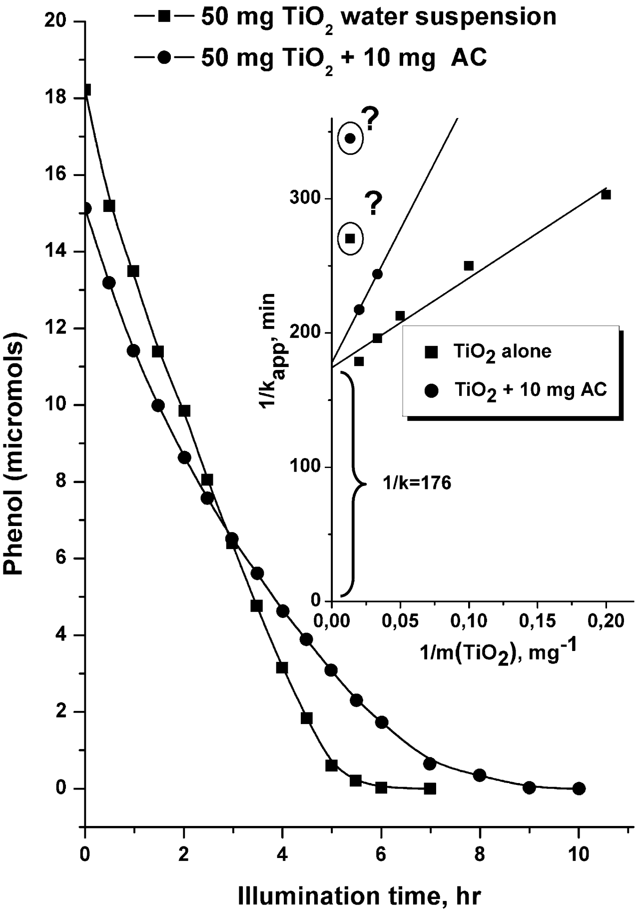

Fig. 6. Kinetic curves of phenol photocatalytic decomposition in water suspension reported in [14]. (■) 50 mg of TiO_2 in ≈100 ml water suspension; (●) 50 mg of TiO_2 and 10 mg of activated carbon in ≈100 ml water suspension. The inset shows dependences of apparent first-order kinetic constants on the amount of TiO_2 in water suspension: (■) varying of TiO_2 quantity; (●) varying of TiO_2 quantity in the presence of 10 mg of activated carbon.

Taking into account, that the total change of substrate (A) amount in the reactor is determined by its inlet and (P) outlet and surface reaction and the total change of product amount is determined by its outlet and surface reaction the system of two differential equations could be suggested:

$$\begin{cases} \dfrac{d}{dt}\left(A + \dfrac{S_\Sigma}{V}(C_{a1} + C_{a2})\right) = \dfrac{A_0 - A}{\tau} - \dfrac{S_\Sigma}{V} k \dfrac{C_1 K_{a1} A}{1 + K_{a1} A} \\ \dfrac{dP}{dt} = \alpha \dfrac{S_\Sigma}{V} k \dfrac{C_1 K_{a1} A}{1 + K_{a1} A} - \dfrac{P}{\tau} \end{cases} \tag{14}$$

Substituting Eq. (4) and (5) into Eq. (14) and rearranging gives:

$$\begin{cases} \dfrac{dA}{dt} = \dfrac{(A_0 - A)/\tau - (S_\Sigma/V) k (C_1 K_{a1} A/(1 + K_{a1} A))}{1 + (S_\Sigma/V)\left[(C_1 K_{a1}/(1 + K_{a1} A)^2) + (C_2 K_{a2}/(1 + K_{a2} A)^2)\right]} \\ \dfrac{dP}{dt} = \alpha \dfrac{S_\Sigma}{V} k \dfrac{C_1 K_{a1} A}{1 + K_{a1} A} - \dfrac{P}{\tau} \end{cases} \tag{15}$$

In the steady state when the right-hand sides of the equations set (15) equal zero the adsorbent does not influence on the substrate (A) and product (P) steady state concentrations at all because adsorbent parameters are only in the denominator. But the process of achieving the steady state is affected by the adsorbent.

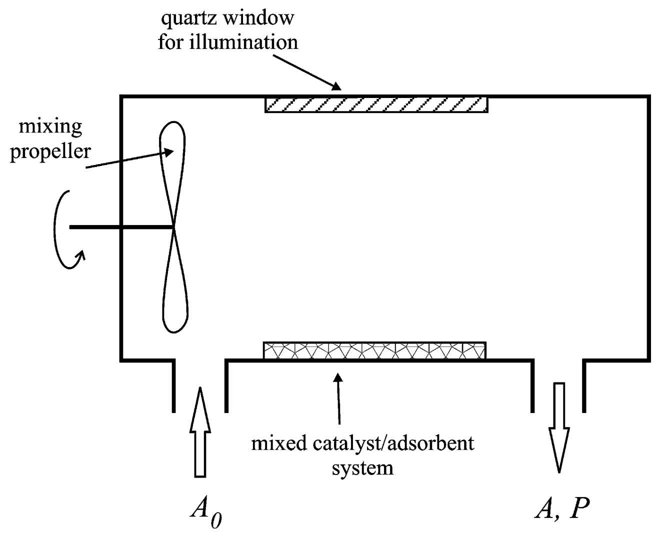

Fig. 7. Flow reactor with ideal mixing (not real construction). A_0 is inlet substrate concentration. A and P are substrate and product concentrations correspondingly which are equal throughout the reactor volume. Reaction mechanism is corresponding to (S.1).

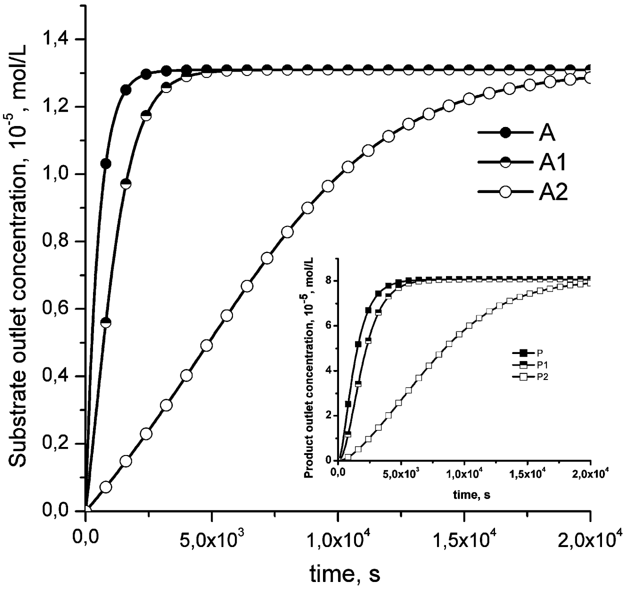

Fig. 8. Calculated kinetic curves for acetone (A) and CO_2 (P) outlet concentrations during the PCO of $A_0 = 4 \times 10^{-5}$ mol l^{-1} inlet acetone concentration in the 0.5 l flow reactor ($u = 30$ cm^3 min^{-1}) with $m_1 = 0.01$ g photocatalyst quantity. Three different cases are presented: (A, P) without adsorbent; (A1, P1) $m_2 = 0.01$ g; (A2, P2) $m_2 = 0.1$ g.

Let the experimental conditions be the same as in Section 2.2, i.e. reactor volume $V = 0.5$ l, catalyst quantity $m_1 = 0.01$ g, inlet substrate concentration $A_0 = 4 \times 10^{-5}$ mol l^{-1} and the contact time $\tau = 1000$ s ($u = 5 \times 10^{-4}$ l s^{-1} or 30 cm^3 min^{-1}). Calculated kinetic curves for three different adsorbent quantities namely $m_2 = 0$; 0.01; 0.1 g are presented in Fig. 8.

The substrate (A) and product (P) concentrations almost achieved steady state levels in all three cases. Steady state concentrations do not depend on the adsorbent quantity as it follows from the equations set (15). They could be found analytically by the solving of third order equation on the A_{ss} concentration and are equal $A_{ss} = 1.3 \times 10^{-5}$ mol l^{-1} and $P_{ss} = 8 \times 10^{-5}$ M. But the time τ_{ss} which is necessary to achieve steady state is increasing with the increase of adsorbent quantity from 1730 s ($m_2 = 0$) through 3330 s ($m_2 = 0.01$ g) till 1.75×10^4 s in the case of $m_2 = 0.1$ g. Especially τ_{ss} becomes huge in the third case when the quantity of adsorbent adsorption sites $N_2 = 2.2 \times 10^{-4}$ mol is almost 10 times higher than the quantity of catalyst active sites $N_1 = 2.9 \times 10^{-5}$ mol. The prolonged kinetics of substrate (A) in the outlet of the reactor in the last case could be used in practice in the case of strong and fast changes of inlet substrate concentration (A_0).

The situation when the A_0 changes from 0 to 4×10^{-5} mol l^{-1} value with the 5000 s time period is shown in Fig. 9. In the case of pure (photo)catalyst the half period 2500 s time is enough to reach steady state in substrate concentration (A) that is why its concentration in the outlet of the system varying from 0 till $A_{ss} = 1.3 \times 10^{-5}$ mol l^{-1} values. Almost the same situation is observing with the low ($m_2 = 0.01$ g) adsorbent quantity when the lowest and highest A_{out} concentrations after 100 periods are equal to 1.4×10^{-6} and 1.22×10^{-5} mol l^{-1}. The most pronounced situation is in the third case when minimum and maximum A_{out} concentrations are equal to 5×10^{-6} and 7.7×10^{-6} mol l^{-1}. Thus the maximum outlet concentration was decreased from $A_{ss} = 1.3 \times 10^{-5}$ till 7.7×10^{-6} mol l^{-1} which equals to 41% from A_{ss} value by simple increase of adsorbent amount.

In practice it means that every time when we have to use small photocatalytic devices due to space limit for example in car cabin and still have a risk of high concentrations of dangerous species we should use mixed (photo)catalyst/adsorbent system because adsorbent will work at the time when catalyst will be in the situation of maximal but insufficient (photo)oxidation rate thus lowering the outlet concentration and minimizing health damage.

On the other hand the adsorbent usage leads to the decrease of the total amount of converted substrate for the same period of time. For example, the total amount of produced CO_2 in three cases

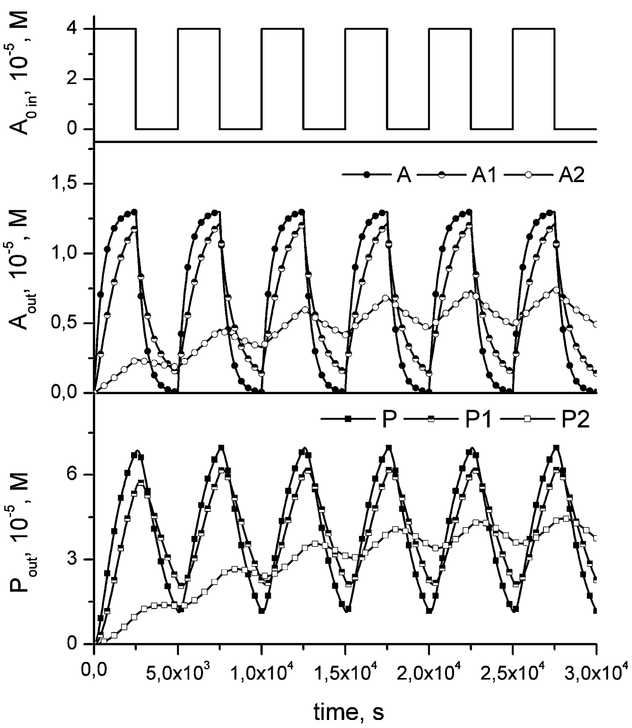

Fig. 9. Calculated kinetic curves for acetone (A) and CO_2 (P) outlet concentrations during the PCO of $A_0 = 4 \times 10^{-5}$ mol l^{-1} inlet acetone concentration which is pulsating with the 5000 s time period in the 0.5 l flow reactor ($u = 30$ cm^3 min^{-1}) with $m_1 = 0.01$ g photocatalyst quantity. The inlet acetone concentration (A_0) profile is presented on the upper graph. Three different cases are presented: (A, P) without adsorbent; (A1, P1) $m_2 = 0.01$ g; (A2, P2) $m_2 = 0.1$ g.

Table 3
Initial parameters for the substrate (A) (photo)catalytic oxidation kinetics simulation in a V = 0.5 l static reactor. Initial substrate concentration is $A_0 = 12 \times 10^{-5}$ mol l^{-1}, stoichiometric factor $\alpha = 3$.

	(Photo)catalyst					Adsorbent					Rate constants			
Parameter	K_{a1}	β_1	S_1	m_1	N_1	K_{a2}	β_2	S_2	m_2	N_1	k_1	k_2	k_3	k_4
Value	1×10^4	8.3×10^{-6}	350	0.01	2.9×10^{-5}	1×10^4	2.8×10^{-6}	800	0.01	2.2×10^{-5}	0.03	0.001	5000	5000

shown in Fig. 9 was estimated by numerical integration of product accumulation kinetic curves for the first 3×10^4 s time period with subsequent multiplication by $u = 5 \times 10^{-4}$ l s^{-1}. Resulted quantities are equal 0.61; 0.60 and 0.44 mmol of produced CO$_2$ for the adsorbent quantity m_2 equal to 0; 0.01 and 0.1 g correspondingly.

3. PCO reaction with intermediate

Current section is devoted to simulation of a double-step photocatalytic reaction in a static reactor. It is supposed that substrate (A) could be adsorbed on the surface of (photo)catalyst and adsorbent whereas product (P) exists only in gaseous form. The intermediate (B) could be moved from the catalyst to the adsorbent surface either through gas phase or through surface bimolecular transfer reaction. It is supposed in the last case that the intermediate (B) exists only in the adsorbed state as it happens if intermediate is a big molecule or if adsorbent has a high adsorptivity against intermediate.

3.1. Intermediate (B) exists only in the adsorbed state

The reaction mechanism (S.2) implies that (photo)catalyst and adsorbent have only one type of surface sites and substrate is adsorbing according to the Langmuir mechanism.

$$\begin{array}{l}
1.\, A + z_1 \overset{K_{a1}}{\rightleftarrows} Az_1 \\
2.\, A + z_2 \overset{K_{a2}}{\rightleftarrows} Az_2 \\
3.\, Az_1 \xrightarrow{k_1} Bz_1 \\
4.\, Bz_1 \xrightarrow{k_2} \alpha P + z_1 \\
5.\, Bz_1 + z_2 \underset{k_4}{\overset{k_3}{\rightleftarrows}} z_1 + Bz_2
\end{array} \qquad \text{(S.2)}$$

The differential and algebraic equations set describing reaction mechanism (S.2) along with the following solution are shown in Appendix B.

Three different cases were simulated with the initial parameters shown in Table 3:

1. Only catalyst is presented in the system with m_1 = 0.01 g;
2. Both catalyst and adsorbent are presented in the system with $m_1 = m_2$ = 0.01 g but the intermediate (B) could not be transferred onto the adsorbent surface ($k_3 = k_4 = 0$);
3. Both catalyst and adsorbent are presented in the system with $m_1 = m_2$ = 0.01 g and the intermediate (B) could be reversibly transferred onto the adsorbent surface (k_3 = 5000, k_4 = 5000).

Ratio $k_3/k_4 = 1$ in the third case means that adsorbent adsorbs intermediate (B) like catalyst. Absolute values were chosen so that reaction 5 from (S.2) could be rated as quasi-equilibrium and higher values of k_3 and k_4 with the same ratio $k_3/k_4 = 1$ did not change shapes of kinetic curves.

In order to underline the adsorbent influence we considered the situation when the rate constant $k_2 \ll k_1$ and there should occur intermediate accumulation on the catalyst surface. The opposite situation $k_2 \gg k_1$ due to the pseudo steady state approximation becomes very similar to the reaction mechanism (S.1). Another important assumption is that initial substrate quantity $A_0V = 5 \times 10^{-5}$ mol is higher than the quantity of catalyst active sites $N_1 = m_1S_1\beta_1 = 2.9 \times 10^{-5}$ mol because only in this case the intermediate (B) could deactivate catalyst appreciably by occupation its surface entirely. Calculated kinetic curves of gas phase and adsorbed species are presented in Figs. 10 and 11 correspondingly.

Like in the case of one-step (photo)catalytic reaction there occur adsorption of substrate before oxidation thus lowering its initial concentration by value $\Delta A_0 = 2.8 \times 10^{-5}$ mol l^{-1} and $\Delta A_s = 4.4 \times 10^{-5}$ mol l^{-1} or by 23% and 37% with only catalyst and with catalyst and adsorbent correspondingly (Fig. 10). Adsorbent influence in this example is less pronounced because the adsorption constant values are equal $K_{a1} = K_{a2} = 1 \times 10^4$ l mol^{-1} (Table 3). Behavior of the substrate (A) and product (P) kinetic curves without adsorbent and with adsorbent but with prohibited surface intermediate transfer is similar with the exception that curve (A2) passes lower then the curve (A1) at the beginning of oxidation due to additional adsorption of gaseous substrate on the adsorbent surface. The effective time of 95% substrate removal from gas phase is equal $t^A_{0.95} = 1450$ s in both cases whereas the analogous time of product accumulation $t^P_{0.95} = 3700$ s.

If to take into consideration the surface intermediate transfer (k_3 = 5000, k_4 = 5000) then the substrate curve (A3) passes much lower with the effective time $t^A_{0.95} = 800$ s but the corresponding product accumulation curve P3 (Fig. 10) has effective time $t^P_{0.95} = 5700$ s due to its overextended tail because the major part of surface intermediate (B) is adsorbed on the (photo)catalytically

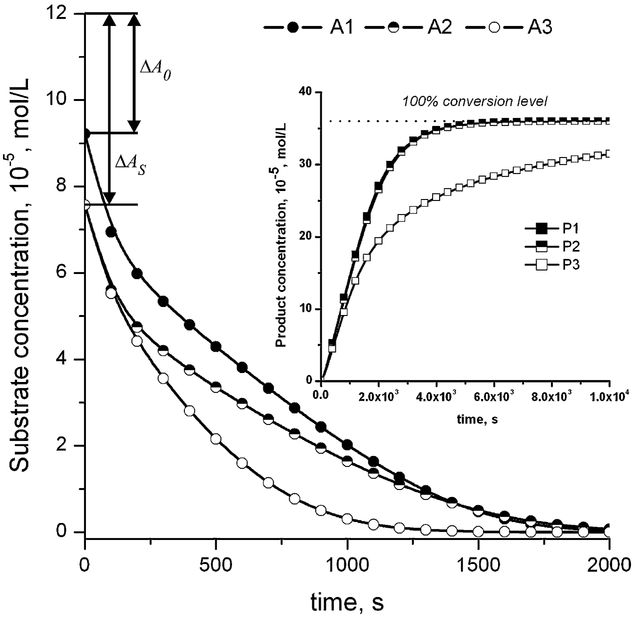

Fig. 10. The adsorbent effect on the kinetics of gaseous substrate (A) removal and product (P) accumulation according to reaction mechanism (S.2) in a 0.5 l static reactor. A1 and P1 are the substrate and product kinetic curves in the system with only (photo)catalyst (m_1 = 0.01 g); A2 and P2 are the substrate and product kinetic curves but in the system with addition of adsorbent (m_2 = 0.01 g) which could not accept intermediate B ($k_3 = k_4 = 0$). A3 and P3 are the same curves in the system with adsorbent (m_2 = 0.01 g) which could accept intermediate B reversibly (k_3 = 5000, k_4 = 5000). All parameters are shown in Table 3.

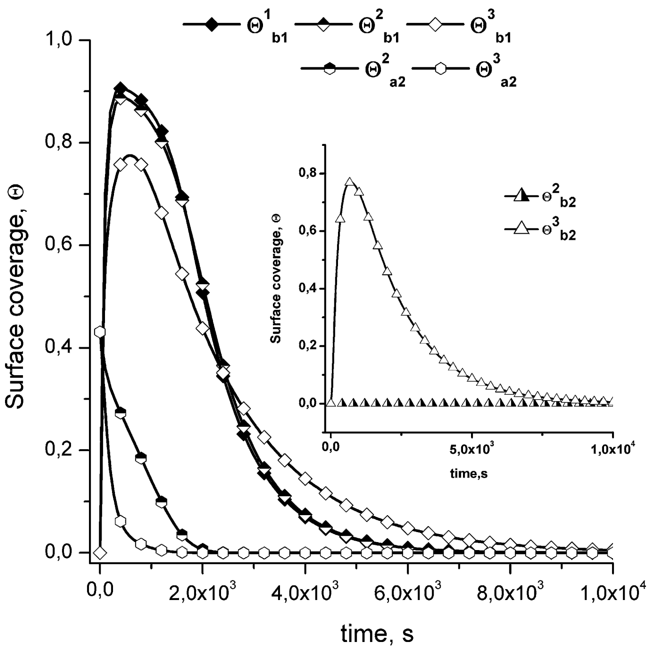

Fig. 11. Dynamics of substrate (A) and intermediate (B) species adsorbed on the surface of catalyst and adsorbent during the same simulation as shown in Fig. 10. Subscript figures correspond to: (1) catalyst; (2) adsorbent. Superscripts correspond to gas phase kinetic curves from Fig. 10: (1) (A1, P1); (2) (A2, P2); (3) (A3, P3).

inactive adsorbent (Fig. 11, curve Θ^3_{b2}) and is slowly involving into the further oxidation (reaction 4, mechanism (S.2)). Behavior of adsorbed surface species (Θ_a and Θ_b, Fig. 11) demonstrates that in the third case the fast formation of adsorbed intermediate and its fast transfer onto the adsorbent surface clear catalyst surface thus keeping higher gaseous substrate removal rate. The maximum adsorbed intermediate coverage $(\Theta_{b2})_{\max}$ is equal to 0.77 and is achieved 700 s after the beginning of oxidation reaction. If one will has to oxidize even higher initial substrate quantity then he has to use higher adsorbent quantity because in current example the $(\Theta_{b2})_{\max}$ value was already close to 1 and additional substrate conversion into adsorbed intermediate (B_{ads}) will be suppressed by its high coverage values of (photo)catalyst and adsorbent surfaces.

3.2. Intermediate (B) could be transferred onto the adsorbent through the gas phase

The reaction mechanism (S.3) implies that (photo)catalyst and adsorbent have only one type of surface sites and substrate and intermediate could adsorb on them according to the competitive Langmuir adsorption mechanism.

$$\begin{array}{l}
1.\, A + z_1 \overset{K_{a1}}{\rightleftarrows} Az_1 \\
2.\, A + z_2 \overset{K_{a2}}{\rightleftarrows} Az_2 \\
3.\, Az_1 \xrightarrow{k_1} Bz_1 \\
4.\, Bz_1 \xrightarrow{k_2} \alpha P + z_1 \\
5.\, B + z_1 \overset{K_{b1}}{\rightleftarrows} Bz_1 \\
6.\, B + z_2 \overset{K_{b2}}{\rightleftarrows} Bz_2
\end{array} \qquad \text{(S.3)}$$

By analogy with the previous case the set of starting differential and algebraic equations along with computations are shown in Appendix C. Here we will discuss only kinetic curves which were calculated for three particular cases (Fig. 12).

It was supposed that both (photo)catalyst and adsorbent have similar adsorption properties against substrate and intermediate ($K_{a1} = K_{a2} = 10^4\ \mathrm{l\ mol^{-1}}$, $K_{b1} = K_{b2} = 10^5\ \mathrm{l\ mol^{-1}}$) and the rate constant k_1 is 10 times higher than k_2 which indicate that intermediate could be accumulated in the reactor and deactivate catalyst.

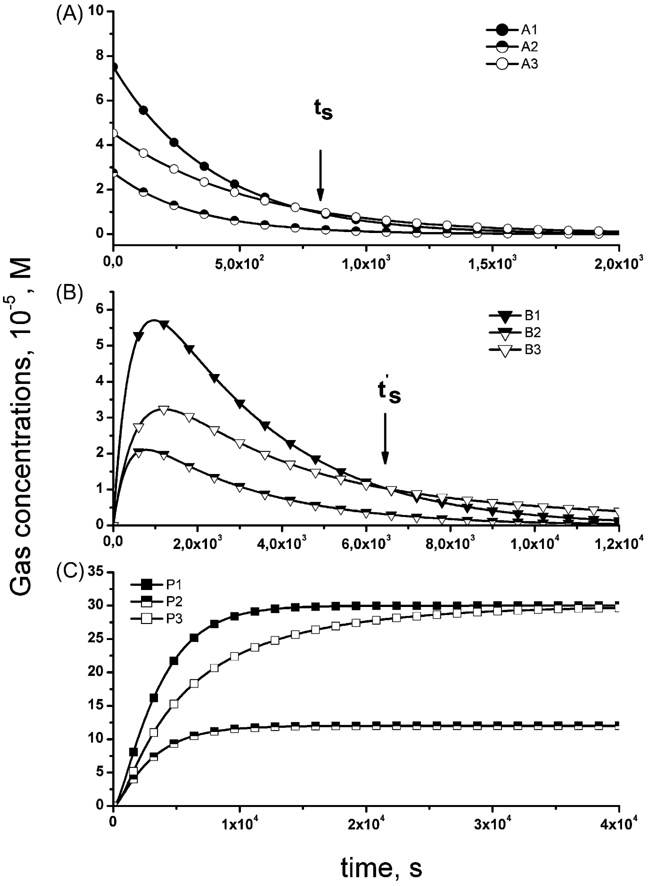

Fig. 12. The initial substrate concentration (A_0) and adsorbent quantity (m_2) influence on the kinetics of substrate (A) (photo)catalytic oxidation according to the reaction mechanism (S.3) in a 0.5 l static reactor. Figures near the substrate (A), intermediate (B) and product (P) labels correspond to: (1) ($A_0 = 10 \times 10^{-5}\ \mathrm{mol\ l^{-1}}$, $m_2 = 0$); (2) ($A_0 = 4 \times 10^{-5}\ \mathrm{mol\ l^{-1}}$, $m_2 = 0$); (3) ($A_0 = 10 \times 10^{-5}\ \mathrm{mol\ l^{-1}}$, $m_2 = 0.01$ g). All other parameters are equal $K_{a1} = K_{b1} = 1 \times 10^4\ \mathrm{l\ mol^{-1}}$, $K_{a2} = K_{b2} = 1 \times 10^5\ \mathrm{l\ mol^{-1}}$, $k_1 = 0.01\ \mathrm{s^{-1}}$, $k_2 = 0.001\ \mathrm{s^{-1}}$, $m_1 = 0.01$ g. Specific surface area and active (adsorption) sites concentrations are the same like in Table 2. Cross-point times: curves A1 and A3, $t_s = 750$ s; curves B1 and B3, $t'_s = 6500$ s.

The substrate (A), intermediate (B) and product (P) kinetic curves behavior at different initial substrate concentrations (A_0) are similar in the reactor without adsorbent (curves 1 and 2, Fig. 12). Although the effective PCO time is slightly higher in the case of $A_0 = 10 \times 10^{-5}\ \mathrm{mol\ l^{-1}}$ but in both cases it takes about 1000 s time to remove 95% of initial effective gaseous substrate concentration ($A_{0,eff}$) and ≈9–10 × 10^3 s time to achieve 95% level of substrate conversion measured by product formation ($t^P_{0.95}$). The maximum intermediate concentration ($B_{\max}$) is 0.21 and 0.57 $\mathrm{mmol\ l^{-1}}$ which is corresponding to 53–55% of A_0 (Table 4).

Kinetics behavior differs if to add 0.01 g of adsorbent. On the one hand we simulated the case of high $A_0 = 10 \times 10^{-5}\ \mathrm{mol\ l^{-1}}$ concentration value but some characteristics are if it were a case of low $A_0 = 4 \times 10^{-5}\ \mathrm{mol\ l^{-1}}$ value. Initial effective gaseous substrate concentration $A_{0,eff} = 4.5 \times 10^{-5}\ \mathrm{mol\ l^{-1}}$ indicating that about 55% of initial substrate amount is in adsorbed state in the beginning of PCO. The maximum intermediate concentration $B_{\max}$ is equal $3.2 \times 10^{-5}\ \mathrm{mol\ l^{-1}}$ or 32% of A_0. Although all effective times namely $t^A_{0.95}$, $t^P_{0.95}$ and $t_{\max}$ became longer and equal to 1600, 2.4×10^4 and 1200 s correspondingly (Table 4).

It is essential to note that like in the case of single-stage reaction mechanism there exist cross-point times $t_s = 750$ s and $t'_s = 6500$ s where substrate (A) and intermediate (B) concentrations are equal

Table 4
Characteristics of (photo)catalytic reaction kinetics shown in Fig. 12.

Initial parameters	$A_{0,\mathrm{eff}}$, M	$\Delta A_0/A_0$, %	$t^A_{0.95}$, s	$t^P_{0.95}$, s	$B_{\max}$, mol l^{-1}	$t_{\max}$, s
$A_0 = 4\times10^{-5}$ mol l^{-1}, $m_2 = 0$	2.75×10^{-5}	31	960	8920	2.1×10^{-5}	800
$A_0 = 10\times10^{-5}$ mol l^{-1}, $m_2 = 0$	7.5×10^{-5}	25	1160	9720	5.7×10^{-5}	950
$A_0 = 10\times10^{-5}$ mol l^{-1}, $m_2 = 0.01$ g	4.5×10^{-5}	55	1600	2.4×10^{4}	3.2×10^{-5}	1200

for cases of reaction to be conducted with or without adsorbent. Such behavior is determined by their retention on the catalyst surface and later desorption into the gas phase. In practice it means that at high reaction times values adsorbent containing system will keep higher substrate and intermediate gas concentrations although such excess could be negligible depending on the adsorbent characteristics and quantity.

4. Conclusions

The influence of adsorbent on the kinetics of (photo)catalytic oxidation processes was investigated in a flow and static conditions for three kinetic mechanisms taking into consideration that substrate and intermediate adsorption could be described by Langmuir isotherm.

1. It was demonstrated that the substrate removal and product formation kinetic curves become longer in static conditions in all cases. In other words complete substrate removal requires more time if one will conduct (photo)catalytic process in presence of adsorbent. On the other hand substrate and intermediate concentration in gas or liquid phase become noticeably smaller in the first part of kinetics due to additional adsorption thus decreasing the toxic substrate and intermediate effect.
2. Using the adsorbent in flow conditions could be effective if substrate (A) inlet concentration increases periodically. In this case adsorbent works as buffer reducing the value of maximum substrate outlet concentration in several times.
3. In the case of double-step reaction mechanism the adsorbent reduces maximum intermediate concentration and can decrease the effective time of substrate removal if the intermediate is non-volatile. In this sense adsorbent could decrease the catalyst deactivation because it takes a certain amount of intermediate (B) from catalyst surface thus keeping its activity at appropriate level.

Acknowledgement

The work is supported by Russian Federal Innovation Agency via the program “Scientific and Educational cadres”. One of the authors (D.V.) appreciates the support of the “Russian Science Support Foundation”.

Appendix A. Nomenclature

A,B,P	concentration of substrate, intermediate and product in the gas (or liquid) phase (mol l^{-1})
A_0	initial concentration of substrate in the gas (or liquid) phase (mol l^{-1}) without taking into account its adsorption or inlet substrate concentration
V	volume of the gas (or liquid) phase (l)
k, k_1, k_2	rate constants of monomolecular surface reactions (s^{-1})
k_3, k_4	rate constants of bimolecular surface reactions of intermediate transfer from photocatalyst onto adsorbent and backward (m^2 mol^{-1} s^{-1})
k', k''	apparent first-order rate constants (s^{-1})
K	adsorption constant (l mol^{-1})
N	quantity of active (adsorption) sites (mol)
C	surface concentration of adsorbed species (mol m^{-2})
S_Σ	total surface of photo(catalyst) and adsorbent in the system (m^2)
S_{BET}	specific surface for (photo)catalyst or adsorbent (m^2 g^{-1})
m	mass of adsorbent (g)
t_s	cross-point time (s)
z	surface active (adsorption) site

Subscripts

a	substrate
b	intermediate
ss	steady state concentrations of substrate and product in the outlet of the reactor
out	concentration in the outlet of a reactor
1	(photo)catalyst, except for the rate constants
2	adsorbent, except for the rate constants

Greek letters

α	a number of product molecules forming from one substrate molecule
β	specific concentration of surface sites (mol m^{-2})
Θ	surface coverage
τ	contact time (s)
τ_{ss}	steady state transient period (s), when substrate current concentration $A = 0.95 \times A_{ss}$

Appendix B. Mathematical formulation of reaction mechanism S.2

$$\begin{aligned}
&1.\ A + z_1 \overset{K_{a1}}{\rightleftarrows} Az_1\\
&2.\ A + z_2 \overset{K_{a2}}{\rightleftarrows} Az_2\\
&3.\ Az_1 \xrightarrow{k_1} Bz_1 \qquad\qquad \text{Reaction mechanism (S.2)}\\
&4.\ Bz_1 \xrightarrow{k_2} \alpha P + z_1\\
&5.\ Bz_1 + z_2 \underset{k_4}{\overset{k_3}{\rightleftarrows}} z_1 + Bz_2
\end{aligned}$$

Taking into account the total mass balance, substrate adsorption, gaseous product and adsorbed intermediate formation the following equations set could be proposed:

$$A_0V = AV + \frac{PV}{\alpha} + S_\Sigma(C_{a1} + C_{a2} + C_{b1} + C_{b2}) \tag{A.1}$$

$$\frac{dC_{b1}}{dt} = k_1C_{a1} - k_2C_{b1} - k_3C_{b1}(C_2 - C_{a2} - C_{b2}) + k_4(C_1 - C_{a1} - C_{b1})C_{b2} \tag{A.2}$$

$$\frac{dC_{b2}}{dt} = k_3C_{b1}(C_2 - C_{a2} - C_{b2}) - k_4(C_1 - C_{a1} - C_{b1})C_{b2} \tag{A.3}$$

$$\frac{dP}{dt} = \alpha k_2 \frac{S_\Sigma}{V} C_{b1} \tag{A.4}$$

$$C_{a1} = \frac{K_{a1}A(C_1 - C_{b1})}{1 + K_{a1}A}, C_{a2} = \frac{K_{a2}A(C_2 - C_{b2})}{1 + K_{a2}A} \tag{A.5}$$

Eq. (A.1) describes the total mass balance indicating that the initial amount of substrate (A_0) could be in gaseous form of A and P or in the form of adsorbed substrate (C_{a1}, C_{a2}) and intermediate (C_{b1}, C_{b2}). Eq. (A.2) and (A.3) describe the change of intermediate surface concentrations resulting from (photo)catalytic reactions ((S.2)—(3) and (4)) and surface transfer ((S.2)—(5)). Eq. (A.5) describe the substrate Langmuir adsorption taking into account that not the entire catalyst and adsorbent surfaces are available for adsorption desorption processes but minus such occupied with intermediate (C_{b1} or C_{b2}).

Substituting Eq. (A.5) into Eq. (A.1)–(A.3), subsequent differentiation of Eq. (A.1) substituting into the result Eq. (A.2)–(A.4) and final rearranging gives the set of differential equations in $A(t)$, $C_{b1}(t)$ and $C_{b2}(t)$ describing changes of gaseous substrate (A) and surface intermediate (C_{b1} and C_{b2}) concentrations during PCO reaction in a static reactor of V (l) volume.

$$C_{a2} = \frac{C_2 K_{a2}A}{1 + K_{a2}A + K_{b2}B}, C_{b2} = \frac{C_2 K_{b2}A}{1 + K_{a2}A + K_{b2}B} \tag{A.9}$$

This set of equations along with Eq. (A.1) (Appendix B) is completely describing all the processes in the static reactor during PCO reaction namely: Eq. (A.1) – mass balance; Eq. (A.6) – product formation; Eq. (A.7) – intermediate transformations; Eqs. (A.8) and (A.9) – competitive adsorption.

Differentiating Eq. (A.1) (Appendix B) and (A.7) with the following substituting and rearrangement gives the system of two first-order differential equations on substrate (A) and intermediate (B) gas concentrations:

$$\begin{cases} \dfrac{dA}{dt} = f(A,B) \\ \dfrac{dB}{dt} = f'(A,B) \end{cases} \tag{A.10}$$

$$\begin{cases} \dfrac{dA}{dt} = -A\dfrac{\begin{array}{c} k_3 C_{b1}(C_2 - C_{b2})\left[(K_{a1}/((1+K_{a1}A)(1+K_{a2}A))) - (K_{a2}/(1+K_{a2}A)^2)\right] \\ + k_4 C_{b2}(C_1 - C_{b1})\left[(K_{a2}/((1+K_{a1}A)(1+K_{a2}A))) - (K_{a1}/(1+K_{a2}A)^2)\right] + (K_{a1}/(1+K_{a1}A)^2)[k_1(C_1 - C_{b1}) + k_2 C_{b1}(1+K_{a1}A)] \end{array}}{(V/S_\Sigma) + (K_{a1}(C_1 - C_{b1})/(1+K_{a1}A)^2) + (K_{a2}(C_2 - C_{b2})/(1+K_{a2}A)^2)} \\ \dfrac{dC_{b1}}{dt} = (k_1 K_{a1}A + k_4 C_{b2})\dfrac{C_1 - C_{b1}}{1+K_{a1}A} - C_{b1}\left(k_1 + k_3\dfrac{C_2 - C_{b2}}{1+K_{a2}A}\right) \\ \dfrac{dC_{b2}}{dt} = k_3 C_{b1}\left(\dfrac{C_2 - C_{b2}}{1+K_{a2}A}\right) - k_4 C_{b2}\left(\dfrac{C_1 - C_{b1}}{1+K_{a1}A}\right) \end{cases}$$

Appendix C. Mathematical formulation of reaction mechanism S.3

$1.\ A + z_1 \overset{K_{a1}}{\rightleftarrows} Az_1$

$2.\ A + z_2 \overset{K_{a2}}{\rightleftarrows} Az_2$

$3.\ Az_1 \xrightarrow{k_1} Bz_1$

$4.\ Bz_1 \xrightarrow{k_2} \alpha P + z_1$

$5.\ B + z_1 \overset{K_{b1}}{\rightleftarrows} Bz_1$

$6.\ B + z_2 \overset{K_{b2}}{\rightleftarrows} Bz_2$

Reaction mechanism (S.3)

By analogy with the previous case the following set of differential and algebraic equations could be proposed:

$$\frac{dP}{dt} = \alpha k_2 \frac{S_\Sigma}{V} C_{b1} \tag{A.6}$$

$$\frac{d}{dt}\left(B + \frac{S_\Sigma}{V}(C_{b1} + C_{b2})\right) = \frac{S_\Sigma}{V}(k_1 C_{a1} - k_2 C_{b1}) \tag{A.7}$$

$$C_{a1} = \frac{C_1 K_{a1}A}{1 + K_{a1}A + K_{b1}B}, C_{b1} = \frac{C_1 K_{b1}A}{1 + K_{a1}A + K_{b1}B} \tag{A.8}$$

References

[1] D.F. Ollis, H. Al-Ekabi (Eds.), Photocatalytic Purification and Treatment of Water and Air, Elsevier, 1993.
[2] A. Fujishima, T.N. Rao, D.A. Tryk, J. Photochem. Photobiol. C 1 (2000) 1–21.
[3] Kaneko Masao, Okura Ichiro, Photocatalysis: Science and Technology, Springer, 2002.
[4] O. Carp, C.L. Huisman, A. Reller, Prog. Solid State Chem. 32 (2004) 33–177.
[5] M.L. Sauer, D.F. Ollis, J. Catal. 149 (1994) 81–91.
[6] A.V. Vorontsov, E.N. Savinov, Chem. Eng. J. 70 (1998) 231–235.
[7] P. Monneyron, M.-H. Manero, J.-N. Foussard, F. Benoit-Marquié, M.-T. Maurette, Chem. Eng. Sci. 58 (2003) 971–978.
[8] F. Shiraishi, S. Yamaguchi, Y. Ohbuchi, Chem. Eng. Sci. 58 (2003) 929–934.
[9] P. Chin, L.P. Yang, D.F. Ollis, J. Catal. 237 (2006) 29–37.
[10] C.H. Ao, S.C. Lee, Chem. Eng. Sci. 60 (2005) 103–109.
[11] D.F. Ollis, J. Phys. Chem. B 109 (2005) 2439–2444.
[12] A. Mills, J. Wang, D.F. Ollis, J. Catal. 243 (2006) 1–6.
[13] A.V. Vorontsov, D.V. Kozlov, P.G. Smirniotis, V.N. Parmon, Kinet. Catal. 46 (3) (2005) 422–436.
[14] J. Matos, J. Laine, J.-M. Herrmann, J. Catal. 200 (2001) 10–20.
[15] J.-M. Herrmann, J. Matos, J. Disdier, Ch. Guillard, J. Laine, S. Malato, J. Blanco, Catal. Today 54 (1999) 255–265.
[16] J. Matos, J. Laine, J.-M. Herrmann, D. Uzcatequi, J.L. Brito, Appl. Catal. B 70 (2007) 461–469.
[17] M. Takeuchi, J. Deguchi, M. Hidaka, Sh. Sakai, K. Woo, P.-P. Choi, J.-K. Park, M. Anpo, Appl. Catal. B 89 (2009) 406–410.
[18] M.S. Vohra, K. Tanaka, Environ. Sci. Technol. 35 (2001) 411–415.
[19] M.L. Sauer, D.F. Ollis, J. Catal. 163 (1996) 215–217.
[20] T. Jiun-Horng, C. Hsui-Mei, H. Guan-Yinag, C. Hung-Lung, J. Hazard. Mater. 154 (2008) 1183–1191.
[21] A.V. Vorontsov, I.V. Stoyanova, D.V. Kozlov, V.I. Simagina, E.N. Savinov, J. Catal. 189 (2000) 360–369.